Zeigler, K.E., Heckert, A.B., and Lucas, S.G., eds., 2003, Paleontology and Geology of the Snyder Quarry, New Mexico Museum of Natural History and Science Bulletin No. 24.

AN ILLUSTRATED ATLAS OF THE PHYTOSAUR (ARCHOSAURIA: PARASUCHIDAE) POSTCRANIA FROM THE UPPER TRIASSIC SNYDER QUARRY (PETRIFIED FOREST FORMATION, CHINLE GROUP)

KATE E. ZEIGLER, ANDREW B. HECKERT and SPENCER G. LUCAS

New Mexico Museum of Natural History, 1801 Mountain Road NW, Albuquerque, NM 87104-1375

Abstract—The Upper Triassic Snyder quarry of north-central New Mexico yields the remains of numerous individuals of the phytosaur *Pseudopalatus buceros*, as well as other vertebrates. The majority of the phytosaurian skeletal elements in the quarry are associated with skulls, so the phytosaur postcrania are clearly those of *P. buceros*. We describe the postcranial material of *P. buceros*, with accompanying illustrations and metrics. In examining this suite of postcranial material, it is apparent that sexual dimorphism in *P. buceros* is restricted solely to the skull, as none of the postcrania differ substantially. There is no obvious quantitative relationship between length of any given appendicular element and its midshaft width, though it appears that the midshaft width may increase more than the length, leading to a more robust bone in adults. This thickening of the midshaft could aid in supporting the weight of an adult animal.

Keywords: Parasuchidae, archosaur, postcrania, dimorphism, phytosaur

INTRODUCTION

Phytosaurs, large, semi-aquatic archosaurs, are common fossils known from Late Triassic sediments worldwide (Gregory, 1962; Westphal, 1976; Hunt, 1994; Long and Murry, 1995; Hungerbühler, 2002). Fossil material of these crocodile-like animals has been recovered from Triassic rocks of the American Southwest since the late 1800s (Cope, 1881). In the Chama basin of north-central New Mexico, phytosaur fossils are quite common (Cope, 1881; Huene, 1915; Lucas and Hunt, 1992; Hunt and Lucas, 1993). In fact, the single largest accumulation of phytosaurs yet discovered (MNI = 20+), the Canjilon quarry, lies near Ghost Ranch in the eastern half of the basin (Lawler, 1974; Long et al., 1989; Hunt and Downs, 2002; Martz, 2002a,b; Zeigler et al., 2002b). The Snyder quarry, which is stratigraphically equivalent to the Canjilon quarry, also contains a large concentration of associated phytosaur material representing at least 11 individuals (Zeigler, 2002; Zeigler et al., 2002a). Very few authors have chosen to describe phytosaur postcranial material, usually because postcranial elements are dissociated from the skulls that are more commonly described. Here we describe the phytosaur skeletal material from the Snyder quarry and discuss sexual dimorphism and ontogeny in phytosaurs.

The Snyder quarry assemblage is important because it appears to represent a life assemblage, effectively preserving a snapshot of an ecosystem (Zeigler, 2002, 2003). As such, it presents a rare opportunity to sample a single population of phytosaurs. Presently we know from excavating all or part of 11 skulls that there were at least 11 phytosaurs represented in this assemblage. For most of the postcranial elements we describe here, there are at least seven specimens available and, even after accounting for possible paired elements, the minimum number of individuals (MNI) represented is typically at least five.

Relatively little systematic work has been performed on phytosaur postcrania. Consequently, all of the diverse phytosaur taxonomies proposed in the last half-century rely almost entirely on characters of the skull, often to the exclusion of the lower jaw (Gregory, 1962; Westphal, 1976; Ballew, 1989; Hunt, 1994; Long and Murry, 1995; Hungerbühler, 1998, 2002). Indeed, the only phytosaur taxonomic schemes that make substantive use of postcranial features are Camp (1930) and Hunt (1994), and both of these really only add a few distinctive features of the pelvic girdle, particularly the ilium.

STRATIGRAPHY AND AGE

The Snyder quarry is stratigraphically high in the Painted Desert Member of the Petrified Forest Formation (Fig. 1). Although the Triassic stratigraphy of the Chama basin is treated in greater detail elsewhere in this volume (Lucas et al., 2003), the stratigraphic position of the Snyder quarry is noteworthy for several reasons with respect to phytosaur systematics.

The Snyder quarry is stratigraphically equivalent to the Canjilon quarry, the largest known sample of phytosaurs yet documented (Lawler, 1974; Long et al., 1989; Zeigler et al., 2002b; Hunt and Downs, 2002). Because the two quarries are at the same horizon and include the same taxon, *Pseudopalatus buceros*, we are optimistic that, eventually, data from both may yield additional insight into the biology of *Pseudopalatus*. We feel that this extrapolation is justified because the two quarries are at the same stratigraphic level, preserve the same taxa, and may well have been formed during the aftermath of the same catastrophic event (Zeigler, 2002; Zeigler et al., 2002b).

Another feature of the Snyder quarry is its relatively high stratigraphic position. Indeed, almost all specimens of *Pseudopalatus* from the Chama basin appear to come from a stratigraphic position somewhat higher in Revueltian-aged strata than the bulk of the other *Pseudopalatus* specimens, namely those from the Bull Canyon Formation of east-central New Mexico (Hunt, 1994; Long and Murry, 1995), and the lower Painted Desert Member of the Petrified Forest Formation in Petrified Forest National Park (=*Machaeroprosopus tenuis* of Camp, 1930; *Pseudopalatus* of Hunt, 1994, and Long and Murry, 1995). Indeed, the only stratigraphically higher specimens of *Pseudopalatus* we are aware of are those from the Owl Rock Formation reported by Kirby (1989, 1991, 1993) (Heckert and Lucas, 2000). Thus, it may eventually be possible to document anagenetic evolution in *Pseudopalatus* by comparing specimens from diverse stratigraphic levels.

Finally, the Snyder quarry is, as the preceeding text documents, squarely in the middle of the stratigraphic range representing the Revueltian land-vertebrate faunachron. *Pseudopalatus* is an index taxon of the Revueltian and if we or another researcher can document taxonomically significant features in the postcrania, this will help other workers to identify *Pseudopalatus* from material more fragmentary than

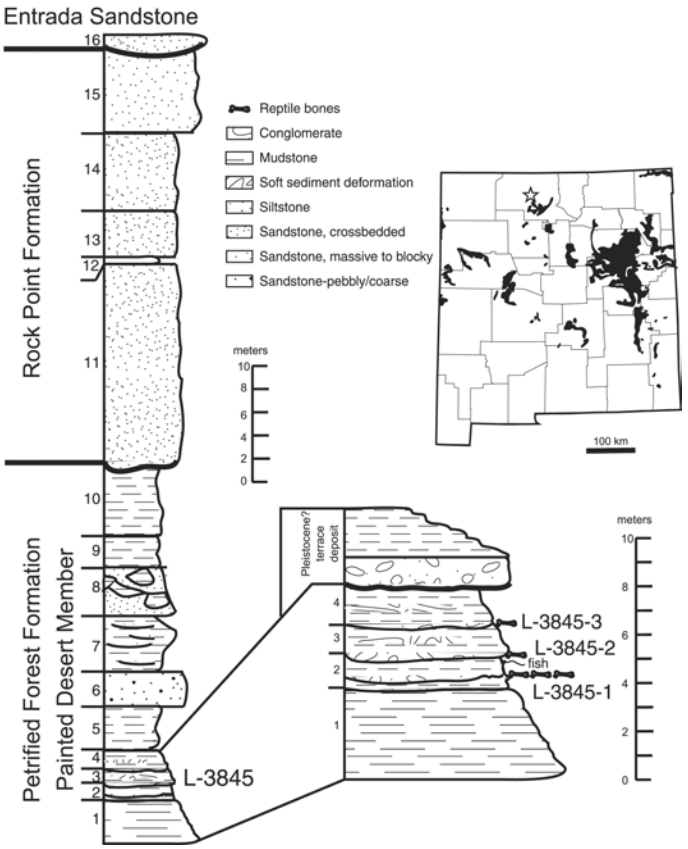

FIGURE 1. Index map showing location of the Snyder quarry site in north-central New Mexico, distribution of Triassic outcrops (from Heckert et al., 2000), and stratigraphic section at the quarry.

the nearly complete skulls required to identify phytosaurs in the current taxonomic schemes.

SYSTEMATIC PALEONTOLOGY AND DIAGNOSIS

Order Archosauria

Family Parasuchidae

Genus *Pseudopalatus*

Pseudopalatus buceros

Pseudopalatus is diagnosed by the following features (Long and Murry, 1995): squamosal with a posterior process that is prolonged, narrow dorsoventrally and tapering to a sharp point. The rostrum is slender and very long, so that the rostral length is much greater than that of the posterior portion of the skull. The teeth of *Pseudopalatus* are homodont to weakly heterodont, with well separated alveoli. The parietal-occipital complex is an inverted "u" in outline, as seen in posterior view. The nares are raised above the level of the skull deck (though this may be a taphonomic feature more than a morphological feature). The supratemporal fenestrae are narrow and recessed below the skull deck, and the parietal wings are depressed and concealed in dorsal view. All skulls of *Pseudopalatus* recovered and prepared from the Snyder quarry thus far preserve these features, so we are confident in assigning the Snyder quarry sample to *Pseudopalatus* (e.g., Zeigler et al., 2002a).

SKELETAL DESCRIPTION

In the material recovered from the Snyder quarry, nearly every element of the postcrania is represented (Table 1; see also Appendix 1, 2). Each element is described from a single specimen (more than one in cases where there was no complete specimen available). However, it is important to note that the suite of elements used here is not from a single articulated specimen. These are all postcranial elements that are directly referable to *Pseudopalatus buceros*, as all the material in the quarry was associated with cranial material. Because the material is disarticulated, we make no effort to describe or illustrate the axial skeleton, ribs or gastralia.

Pectoral Girdle

The best-preserved scapula, a left (NMMNH P-35998), is a gracile bone that is 258 mm tall, 88 mm anterior-posteriorly long at the base, 70 mm anterior-posteriorly across the top of the blade, and the widest articular facet (for the coracoid) is 53 mm wide (Fig. 2B, 3B). The scapular blade curves gently posteriorly with a gentle flexure medially and is extremely thin (<0.3 mm). The blade thickens moderately both lateromedially and anteroposteriorly about halfway down its length. The posterior edge of the blade is a smooth curve down into the glenoid and coracoid articulations (versus McGregor's "*Rhytiodon*," [=*Rutiodon*] 1906). There is a somewhat abrupt flare laterally and posteriorly for the glenoid, which is the articular surface for the humeral head. This laterally-directed process is 28 mm long and is much shorter than is indicated in *Machaeroprosopus* (=*Rutiodon*) as described by Camp (1930). There is also a longer, less abrupt flare medially and posteriorly for articulation with the coracoid. This process is more ventrally directed than illustrated for Camp's (1930) *Machaeroprosopus*. Just above the posterolateral prominence of the glenoid, a small fossa is located approximately 10 mm above the lip of the glenoid. The acromion process is in the anteroventral corner and is very thin (1-2 mm) and blade-like. It is a very distinct rounded lobe/blade that protrudes 10-15 mm farther anteriorly than the widest portion of the blade (versus *Parasuchus*: Chatterjee, 1978). The articular surface as a whole is trilobate, with a rounded lobe laterally (glenoid lip), a more angular lobe medially and a triangular lobe anteriorly. The last two lobes are for articulation with the coracoid and cervical vertebrae.

A well-preservesd left coracoid (NMMNH P-37889) is a nearly complete bone that is long and short, with a deep, rounded ventral blade (Fig. 2F, 3F). It is 88 mm long, 75 mm tall, and ranges in thickness from 2 mm at the ventral margin to 27 mm at the widest point of the articular surface. The articular surface is 53 mm long. The anterior margin has a circular notch, the coracoid notch, and is also an extremely thin, semi-circular blade. The anterior margin of the dorsal surface, including the articular surface, thickens through the curve of the coracoid notch to the anteriormost articular facet. The ventral blade is deeply convex and deepens further towards the anterior end. At the posterior aspect of the coracoid, the glenoid lip drops abruptly ventrally to the beginning of the blade that projects posteriorly and is thicker than the more ventral parts of the blade. This transition from the glenoid lip to the blade forms a right-angle notch, and the posterior edge of the projection is moderately rugose. The articular surface, on the dorsal aspect of the coracoid, has three facets. The lateral and posterior facet is dorsally directed and is the ventral margin of the glenoid fossa. The medial and more anterior facet is medially and slightly dorsally directed to articulate with the scapula. The anteriormost facet is approximately triangular, and the anterior tip of this facet is slightly laterally directed. This facet is separated from the posterior facets by a gentle ridge. The glenoid does not appear as deep, nor as well defined, as illustrated for *Parasuchus* (=*Paleorhinus*) (Chatterjee, 1978). The coracoid itself, when compared to Camp's (1930) illustrations of *Machaeroprosopus* (=*Rutiodon*), does not have as deep a medial convexity, the lateral facet does not project as far anteriorly, and the medial facet is not as deeply divided from the lateral facet on the posterior margin.

To this point, we have not yet identified any interclavicles from the Snyder quarry fossils. This is moderately surprising as these are

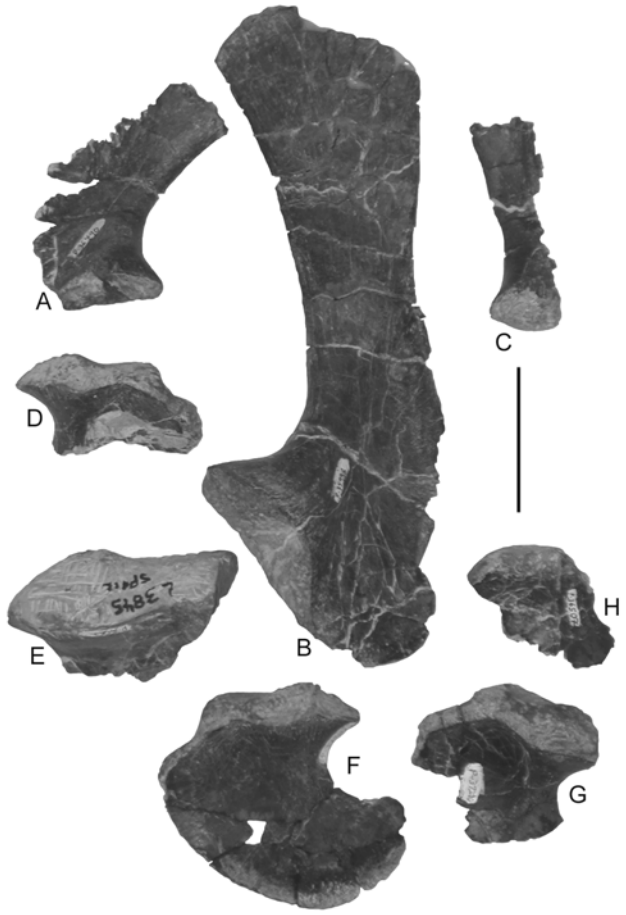

FIGURE 2. Pectoral girdle elements of *Pseudopalatus* from the Snyder quarry in medial view. **A**, NMMNH P-36490, right scapula; **B**, NMMNH P-35998, left scapula; **C**, NMMNH P-35547, left scapula; **D**, NMMNH P-36508, right coracoid; **E**, NMMNH P-36062, right coracoid; **F**, NMMNH P-37889, left coracoid; **G**, NMMNH P-37290, left coracoid; **H**, NMMNH P-36507, left coracoid. Scale bar = 5 cm.

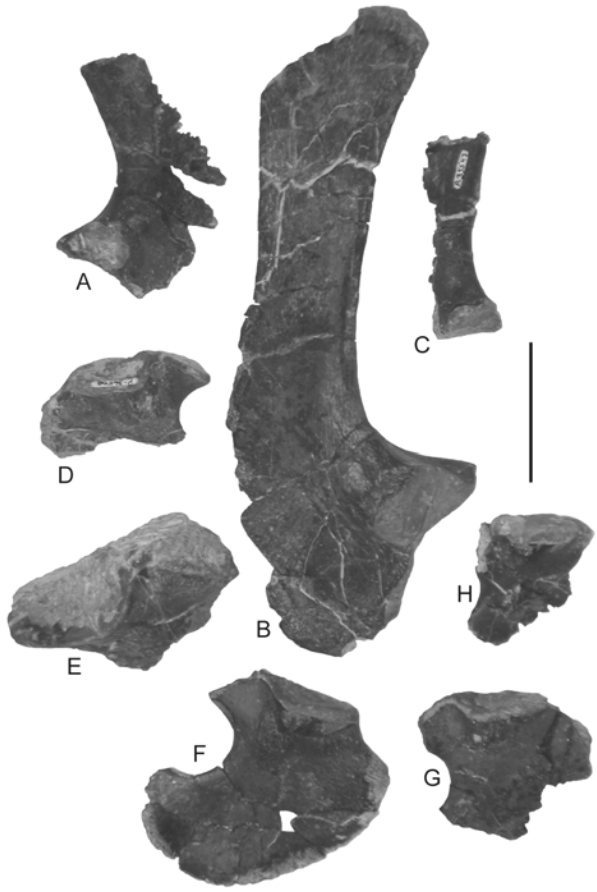

FIGURE 3. Pectoral girdle elements of *Pseudopalatus* from the Snyder quarry in lateral view. **A**, NMMNH P-36490, right scapula; **B**, NMMNH P-35998, left scapula; **C**, NMMNH P-35547, left scapula; **D**, NMMNH P-36508, right coracoid; **E**, NMMNH P-36062, right coracoid; **F**, NMMNH P-37889, left coracoid; **G**, NMMNH P-37290, left coracoid; **H**, NMMNH P-36507, left coracoid. Scale bar = 5 cm.

typically robust elements, although of course only half as many interclavicles are available for fossilization relative to the paired elements.

Forelimb

The best-preserved humerus, a left (NMMNH P-29167), is 250 mm long, with a shaft width of 35 mm, a proximal head width of 99 mm and a distal head width of 81 mm (Fig. 4A, 5A). The proximal end is dorso-ventrally flattened (28 mm thick) with a rugose surface that represents a fused epiphysis. The proximal head dips posteriorly, and the middle of the head is convex, with a slight concavity and abrupt knob on the anterior end. The deltoid crest runs almost along the anterior margin of the ventral surface and is 85 mm long. In some specimens, the crest is broken off so that it forms a gentle ridge. The ventral and dorsal surfaces of the proximal end of the humerus are flat and broad. There is a slight boss or rugosity on the anterior side of the dorsal surface of the proximal end that corresponds to the center of the deltoid crest. The distal end is convex posteriorly and anteriorly with a gentle concavity between these convexities. The posterior convexity is directed posteriorly, whereas the anterior convexity is more distally and laterally directed. The dorsal surface of the distal end is broad and flat, whereas the ventral surface has a slight concavity. There is a well defined radio-condylar/ectepicondylar groove present that is approximately 40 mm long. It begins on the distal anterior edge of the humerus and curves up to the dorsal surface and is parallel to a crest on the anteroventral edge of the distal shaft and is 11 mm at its widest. The humerus is, in general, similar to other described phytosaur humeri (Camp, 1930; Chatterjee, 1978; Long and Murry, 1995), though the deltoid crest is not as sharply defined or recurved as is illustrated for *Machaeroprosopus* (Camp, 1930).

The right ulna (NMMNH P-33295) is 147 mm long, 20 mm wide at mid-shaft, 48 mm across the proximal end and 36 mm across the distal end (Fig. 6C, 7C). The ulna is generally quite flat, though the proximal end swells anteriorly along the medial half of the proximal head and is 18 mm anteroposteriorly. The olecranon process on the medial side of the proximal end is strongly developed and is 7 mm from the epiphysial line to the highest point of the olecranon process. The process slopes sharply medially to a small process at the articular point with the radius, which lies medially to the ulna, and slopes more gently laterally. The medial edge of the shaft is broader anteroposteriorly than the lateral edge, which is more ridge-like. The posterior face of both the proximal and distal ends is broad and flat, whereas the anterior face is broad and flat at the distal end, but swells out below the olecranon process on the proximal end. The distal end flares gently from mid-shaft and is anteroposteriorly flattened. The distal head is slightly convex with moderately well-defined fused epiphyses. The entire ulna is gently curved medially, more sharply so at the proximal end. The ulna is more gracile than illustrated specimens of *Mystriosuchus*

FIGURE 4. Humeri of *Pseudopalatus* from the Snyder quarry in ventral view. **A**, NMMNH P-29167, left; **B**, NMMNH P-34733, left; **C**, NMMNH P-35443, left; **D**, NMMNH P-36057, right; **E**, NMMNH P-34731, right; **F**, NMMNH P-34751, right; **G**, NMMNH P-36069, right. Scale bar = 5 cm.

FIGURE 5. Humeri of *Pseudopalatus* from the Snyder quarry in dorsal view. **A**, NMMNH P-29167, left; **B**, NMMNH P-34733, left; **C**, NMMNH P-35443, left; **D**, NMMNH P-36057, right; **E**, NMMNH P-34731, right; **F**, NMMNH P-34751, right; **G**, NMMNH P-36069, right. Scale bar = 5 cm.

(McGregor, 1906). The distal end does not appear to be at all "swollen" (Chatterjee, 1978), nor is it "very thick and rounded" (Camp, 1930). In fact, the distal end is only 7 mm thick.

The radii consist of a proximal radius fragment (NMMNH P-34749) and a distal radius fragment (NMMNH P-34750). No complete phytosaur radii have yet been recovered from the quarry (Fig. 8). The proximal end is 27 mm mediolaterally, 18 mm anteroposteriorly, 16 mm mediolaterally at midshaft and 12 mm anteroposteriorly at midshaft. The proximal end is thus wider mediolaterally than it is anteroposteriorly and is not completely round. The lateral end of the proximal head has an abrupt process or convexity that is directed more dorsally than laterally, as illustrated in *Parasuchus* (Chatterjee, 1978). The distal end is 23 mm mediolaterally, 20 mm anteroposteriorly, 14 mm mediolaterally at midshaft and 11 mm anterodorsally at midshaft. The distal end is quite round in cross-section, and the shaft swells out slightly into the distal head. The lateral side of the distal end broadens anteroposteriorly with a shallow groove that begins more laterally at its proximal end and curves around to the lateral side of the posterior face. The groove is 35 mm long, and is bordered laterally by a very slight ridge (1 mm high) along the lateral side of the radius. The shaft appears to have a very gentle lateral curve.

Pelvic Girdle

No phytosaur ilia have been sufficiently prepared to be accurately described, and only two (a juvenile and subadult) are known at this time. Only slightly better represented are the pubes (1 specimen, Fig. 9B, 10B) and the ischia (1 specimen, Fig. 9A, 10A)

The pubis is represented by an incomplete right pubis (NMMNH P-37346) that is missing the posteroventral blade (Fig. 9B, 10B). The pubis is 137 mm anteroposteriorly, 47 mm dorsoventrally, 31 mm

FIGURE 6. Ulnae of *Pseudopalatus* from the Snyder quarry in anterior view. **A**, NMMNH P-34756, right; **B**, NMMNH P-35476, right; **C**, NMMNH P-33295, right; **D**, NMMNH P-37810, left; **E**, NMMNH P-29986, left; **F**, NMMNH P-31294, left; **G**, NMMNH P-36410, right; **H**, NMMNH P-39253, right; **I**, NMMNH P-34724, right; **J**, NMMNH P-33292, left; **K**, NMMNH P-39197, left; **L**, NMMNH P-35479, left. Scale bar = 5 cm.

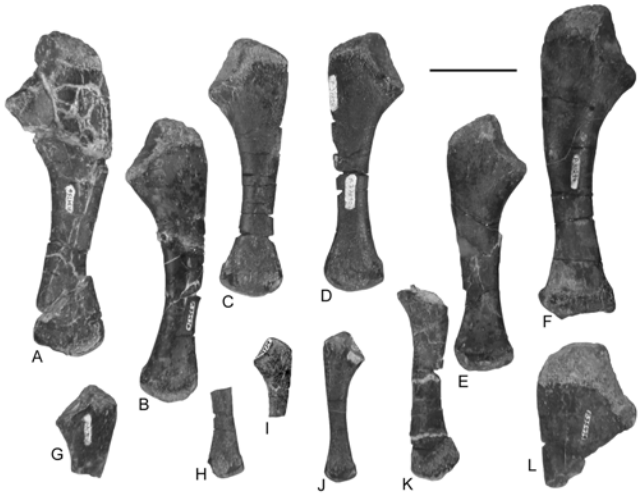

FIGURE 7. Ulnae of *Pseudopalatus* from the Snyder quarry in posterior view. **A**, NMMNH P-34756, right; **B**, NMMNH P-35476, right; **C**, NMMNH P-33295, right; **D**, NMMNH P-37810, left; **E**, NMMNH P-29986, left; **F**, NMMNH P-31294, left; **G**, NMMNH P-36410, right; **H**, NMMNH P-39253, right; **I**, NMMNH P-34724, right; **J**, NMMNH P-33292, left; **K**, NMMNH P-39197, left; **L**, NMMNH P-35479, left. Scale bar = 5 cm.

TABLE 1. List of all phytosaur appendicular elements from the Snyder quarry catalogued as of 2/12/03.

Skeletal Element	Specimen ID	Side	Degree of Completeness
Scapula	P-35998	Left	Complete
	P-35547	Left	Partial - 50% (blade damaged, no acromion proc.)
	P-36490	Right	Partial - 75% (blade damaged, no acromion proc.)
Coracoid	P-37889	Left	Complete
	P-37290	Left	Partial - 50% (only artic. platform)
	P-36507	Left	Partial - 30% (only artic. platform)
	P-36062	Right	Partial - 30% (only artic. platform)
	P-36508	Right	Partial - 30% (only artic. platform)
Humerus	P-34733	Left	Complete
	P-35443	Left	Partial - 40% (only midshaft)
	P-34751	Left	Partial - 75% (no distal end)
	P-29167	Left	Complete
	P-31297	Right	Complete
	P-34731	Right	Complete
	P-36069	Right	Partial - 80% (no distal end)
	P-36057	Right	Partial - 20% (only distal end)
Ulna	P-31294	Left	Complete (pathological)
	P-29986	Left	Complete
	P-33292	Left	Complete
	P-39197	Left	Partial - 80% (no proximal end)
	P-35479	Left	Partial - 20% (only proximal end)
	P-37890	Left	Complete
	P-39253	Left	Partial - 50% (only distal half)
	P-34756	Right	Complete
	P-35476	Right	Complete
	P-34724	Right	Partial - 50% (only proximal half)
	P-33295	Right	Complete
	P-36140	Right	Partial - 30% (only proximal)
Radius	P-34749	Right	Partial - 75% (no distal end, in segments)
	P-34750	Right	Partial - 50% (only distal end)
Pubis	P-37346	Right	Partial - 50% (only central rib)
Ischium	P-34977	Right	Partial - 75% (only central body)
Femur	P-34732	Left	Complete
	P-33663	Left	Complete (pathological)
	P-30843	Left	Complete
	P-37291	Left	Partial - 70% (only distal)
	P-35999	Left	Complete
	P-33670	Left	Complete
	P-34747	Left	Partial - 40% (only shaft)
	P-39362	Right	Partial - 30% (only distal end)
Tibia	P-36489	Left	Partial - 30% (only proximal end)
	P-37286	Left	Partial - 50% (only distal end)
	P-29979a	Right	Partial - 50% (only distal end)
	P-29979b	Right	Partial - 75% (only distal end)
	P-35785	Right	Complete
	P-29978	Right	Partial - 50% (only proximal end)
	P-33669	Right	Partial - 80% (no distal end)
Fibula	P-37358	Left	Complete
	P-39363	Left	Complete
	P-37352	Right	Complete
	P-39364	Right	Partial - 30% (only distal end)
Astrag.	P-33856	Left	Complete
	P-33929	Left	Complete
	P-33928	Right	Complete
	P-33926	Right	Complete
Calcan.	P-34753	Left	Complete
	P-39204	Right	Complete
	P-33930	Right	Partial - 40% (no lateral end)
Metat. V	P-33129		Complete
	P-34728		Complete
	P-35796		Complete

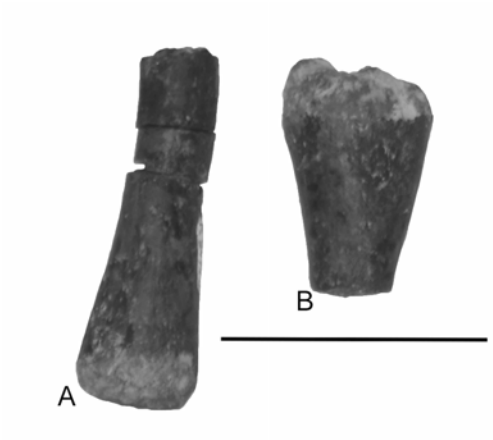

FIGURE 8. Radius fragments of *Pseudopalatus* from the Snyder quarry. **A**, NMMNH P-34749, distal right; **B**, NMMNH P-34750, proximal right. Scale bar = 5 cm.

mediolaterally at the dorsal end, 21 mm mediolaterally in the center of the anterodorsal side, and 10 mm mediolaterally at the anterior end. The anterior edge has a moderately wide articular surface that is a smooth, flat ledge. Anterodorsally, the pubis is much thicker than the ventral and posterior sides. The dorsal/posterior articular surface, including the iliac facet, is badly crushed in this specimen. The ischiatic facet of this articular surface is dorsally directed, and the iliac facet is medially directed. The anterodorsal margin is moderately concave. There is a very small process at the anterior end of the dorsal/anterior margin that is much larger than is illustrated for *Machaeroprosopus* (=*Rutiodon*) (Camp, 1930). The anterior margin of the obturator foramen is preserved at the posterodorsal corner. The overall shape of the pubis does not clearly display the characteristic horizontal articulation of the pubis with the ilium of *Pseudopalatus* (=*M. validus*) (e.g., Camp, 1930; Hunt, 1994).

The ischium is an incomplete right (NMMNH P-34977) that is missing the anterior margin, as well as the posterior ventral projection (Fig. 9A, 10A). It is 122 mm dorsoventrally, 64 mm anteroposteriorly at the dorsal end, 41 mm mediolaterally at the dorsal end, and 8 mm mediolaterally at the ventral end. The anterior margin thins abruptly from a swelling toward the posterior. The posterior half of the dorsal half of the bone has a thick keel running dorso-ventrally. Ventrally, the ischium becomes a thin plate with striations (dorso-ventrally directed) on the ventral edge of the blade. The posterior blade is not present, but the ischium thins towards the posterior projection. The articular face on the dorsal surface has two facets that are not completely discrete. The lateral (ischiatic) facet is dorso-laterally directed to form the ven-

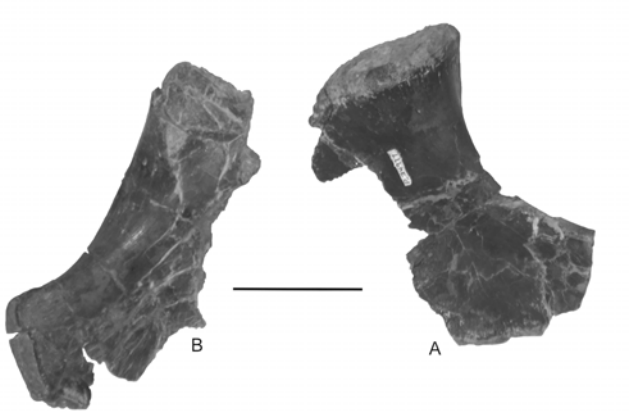

FIGURE 9. Pelvic girdle elements of *Pseudopalatus* from the Snyder quarry in medial view. **A**, NMMNH P-37346, right ischium; **B**, NMMNH P-34977, right pubis. Scale bar = 5 cm.

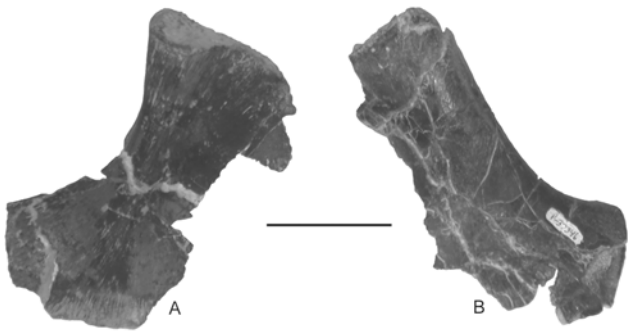

FIGURE 10. Pelvic girdle elements of *Pseudopalatus* from the Snyder quarry in lateral view. **A**, NMMNH P-37346, right ischium; **B**, NMMNH P-34977, right pubis. Scale bar = 5 cm.

tral rim of the acetabulum and is 18 mm mediolaterally and 35 mm anteroposteriorly. The medial facet is much longer than the lateral facet (25 mm mediolaterally and 64 mm anteroposteriorly) and is more dorsally directed.

Hind Limb

The femur (Figs. 11-12), represented by a complete left femur (NMMNH P-30843) is a very long, slender bone with a gentle sigmoidal flexure (Fig. 11B, 12B). The femur is 297 mm long, 34 mm dorsoventrally at midshaft, 77 mm across the proximal head and 64 mm across the distal head. The proximal end is flat and broad with a moderately discrete epiphysis and a gently convex surface. The fourth trochanter, beginning 65 mm below the proximal head, is a rugose ridge in the middle of the ventral side. Directly medial to the fourth trochanter is a moderately rugose muscle scar. Just lateral to the upper half of the fourth trochanter is a similarly rugose surface. On the posterior edge of the shaft, just distal to the fourth trochanter, is a low rugosity (Camp's [1930] "fifth" trochanter). This rugosity is 44 mm long, and near its proximal end, a muscle scar descends down from the posterior face of the bone and intersects the rugosity.

The femoral shaft is long and approximately cylindrical with a slight edge on the posterior side (leading to a nearly "teardrop" cross-section). The posterior edge becomes the ridge of the distal lateral condyle. The distal condyles are somewhat asymmetric, with the lateral condyle being larger and extending farther ventrally than the medial condyle. The medial condyle has a larger ventral articular surface than does the lateral condyle. The intercondylar groove is shallow on the distal surface, and moderately deep on the posteroventral and anterodorsal surfaces. The epiphyses are quite distinct and heavily textured with deep pits and grooves that give the bone surface a wrinkled appearance. The ventral surfaces of the condyles are neither as rough nor as rugose as illustrated by Camp (1930). There is also no large rounded boss on the dorsal surface of the proximal head (e.g., Camp, 1930).

The best preserved tibia (Figs. 13-14) (NMMNH P-35785, right tibia) is 179 mm dorsoventrally, 63 mm anteroposteriorly at the proximal end, 29 mm at mid-shaft and 45 mm at the distal end (Fig. 13A, 14A). The proximal head is greatly expanded in comparison to the distal end, and there is a moderately strong projection of the proximal head anteriorly on the lateral face. The distal end is triangular in outline and is enlarged to the medial side. There are two vaguely defined "condyles" on the distal end. Both articular surfaces, proximal and distal, are convex. There is a slightly developed cnemial crest on the posterior edge of the lateral side that is little more than a rugose patch that is at most 37 mm long. There is a roughened surface on the anterior side of the distal end, representing the point of contact with the distal fibula. The tibia is not as gracile and slender as the other phytosaur limb bones in the assemblage and instead appears relatively short and stout.

The fibula (Figs. 15-16) (NMMNH P-37352, right fibula) is a long, slim bone with a slight sigmoidal flexure (Fig. 15A, 16A). This specimen is 174 mm dorso-ventrally, 28 mm anteroposteriorly at the proximal end, 18 mm at midshaft, and 38 mm at the distal end. It is mediolaterally compressed, not anteroposteriorly as described by Chatterjee (1978). The proximal head is ellipsoid in outline and slightly concave, with a posterior side that projects proximally more than the anterior side. There is a distinct epiphysial line and a very slight swelling on the lateral face just below the this line. The iliofibularis trochanter is approximately halfway down the shaft and is a poorly defined, ovoid rugosity with two separate low bosses, one proximal and one distal. This trochanter is not the large projection described by Chatterjee (1978), nor is it obliquely oriented. Indeed, the fibula figured by Chatterjee (1978) more strongly resembles an aetosaur fibula than a phytosaur fibula. On the NMMNH specimen, there is a faint, much smaller trochanter visible on the posterior surface that is 12 mm long and begins at the same level as the end of the iliofibularis trochanter. Distally, the bone swells anteroposteriorly, is convex, and the posterior side of the head projects farther dorsally. There are not two distinct faces for articulation with the ankle bones. On the anterior edge of the distal end of the bone, a slight ridge is developed that reaches the articular surface. This ridge is moderately rugose and is approximately 11 mm long.

Ankle, Metatarsal V and Unguals

The ankle bones are illustrated in Figs. 17 and 18, while the metatarsals and unguals are illustrated in Figs. 19 and 20. The astragalus we describe is a vaguely cubic bone (NMMNH P-33856, left) that is 41 mm anteroposteriorly, 27 mm mediolaterally at its widest point, and 27 mm dorsoventrally (Fig. 17B, 18B). The dorsal surface is convex posteriorly with an elongate, rounded surface that is moderately rough. The anterior end of the dorsal surface is the saddle for the articulation of the distal tibia, and this articular surface is very smooth. The anterior surface is a subrectangular smooth surface just ventral of the tibial saddle. The ventral surface has an articular facet towards the anterior end for articulation with the underlying metatarsal. This facet is moderately deep, subrectangular and very smooth. Towards the posterior end of the ventral surface, the astragalus protrudes posteriorly and is convex. The posterior surface of the bone is rounded and strongly convex. The medial surface of the astragalus is smooth, concave, and

FIGURE 11. Femora of *Pseudopalatus* from the Snyder quarry in anterodorsal view. **A**, NMMNH P-34732, left; **B**, NMMNH P-30843, left; **C**, NMMNH P-35999, left; **D**, NMMNH P- 33670, left; **E**, NMMNH P-37291, left; **F**, NMMNH P-33663, right; **G**, NMMNH P-34747, right; **H**, NMMNH P-39362, right. Scale bar = 5 cm.

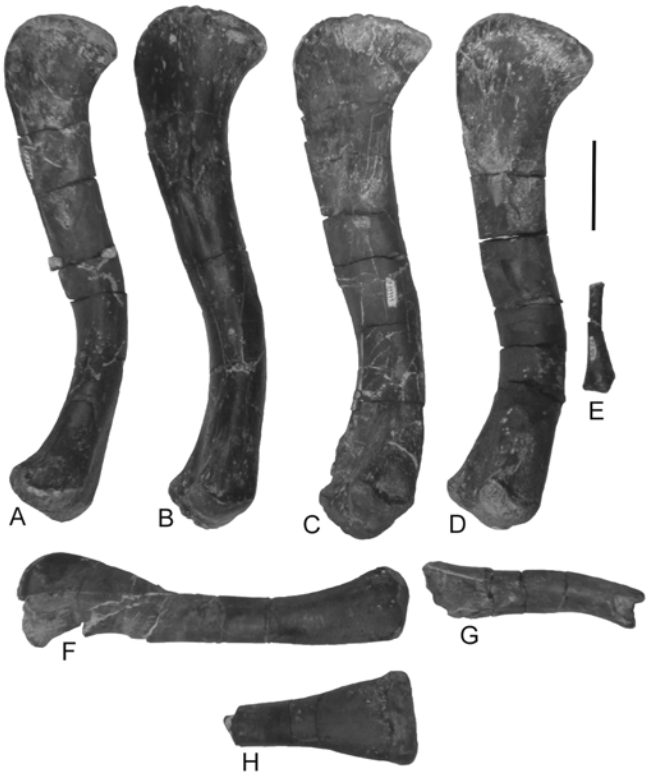

FIGURE 12. Femora of *Pseudopalatus* from the Snyder quarry in posteroventral view. **A**, NMMNH P-34732, left; **B**, NMMNH P-30843, left; **C**, NMMNH P-35999, left; **D**, NMMNH P- 33670, left; **E**, NMMNH P-37291, left; **F**, NMMNH P-33663, right; **G**, NMMNH P-34747, right; **H**, NMMNH P-39362, right. Scale bar = 5 cm.

FIGURE 13. Tibiae of *Pseudopalatus* from the Snyder quarry in medial view. **A**, NMMNH P-35785, right; **B**, NMMNH P-33669, right; **C**, NMMNH P-29979, right; **D**, NMMNH P-29978, right; **E**, NMMNH P-29979, left; **F**, NMMNH P-36489, left; **G**, NMMNH P-37286, left. Scale bar = 5 cm.

FIGURE 14. Tibiae of *Pseudopalatus* from the Snyder quarry in lateral view. **A**, NMMNH P-35785, right; **B**, NMMNH P-33669, right; **C**, NMMNH P-29979, right; **D**, NMMNH P-29978, right; **E**, NMMNH P-29979, left; **F**, NMMNH P-36489, left; **G**, NMMNH P-37286, left. Scale bar = 5 cm.

FIGURE 15. Fibulae of *Pseudopalatus* from the Snyder quarry in medial view. **A**, NMMNH P-37352, right; **B**, NMMNH P-33665, left; **C**, NMMNH P-37358, left. Scale bar = 5 cm.

FIGURE 16. Fibulae of *Pseudopalatus* from the Snyder quarry in lateral view. **A**, NMMNH P-37352, right; **B**, NMMNH P-33665, left; **C**, NMMNH P-37358, left. Scale bar = 5 cm.

ovoid in outline, whereas the lateral surface is moderately smooth, convex and round in outline. The calcaneum articulates with the astragalus against this lateral convexity (e.g. Parrish, 1986).

The calcaneum (NMMNH P-34753, left) is a thin bone with multiple articulation facets (Fig. 17E, 18E). It resembles a metapodial in outline. The calcaneum is 34 mm mediolaterally, 22 mm across the medial end, 14 mm across the lateral end and ranges from 10 to 14 mm anteroposteriorly. The dorsal surface is an elongate saddle that rises medially to the dorsal articular facet on the anterior surface and laterally to the lateral articular surface. The medial anterior surface has two visible facets: the ventral one is ovoid in outline, larger than the more dorsal facet, anteriorly directed and convex. The dorsal facet is approximately ovoid in outline, medially directed (forms the medial surface) and is concave. These two facets are separated by a groove. The midpoint of the bone is concave, and the calcaneum then swells laterally into the lateral articular facet. The ventral surface swells laterally to the lateral articular surface, and medially dips down into a concavity rimmed by the borders of a posterior articular surface and the ventrally-directed anterior facet. The posterior surface laterally swells towards the articular surface and medially becomes a large, flat, triangular articular surface.

Metatarsal V (NMMNH P-34728) is a y-shaped bone that is 65 mm anteroposteriorly, 39 mm mediolaterally at the proximal end, and 18 mm mediolaterally at the distal end (Fig. 19C, 20C). The medial branch of the proximal end flares into a rectangular articular facet, whereas the lateral branch is thin and flat, with a small articular rim on the ventral margin. The distal end flares moderately into an articular facet. On the ventral margin of the lateral aspect, a faint boss is present, approximately halfway along the shaft.

A distal ungual (NMMNH P-35471, left?) is 27 mm anteroposteriorly, 11 mm mediolaterally at the proximal end, 6 mm mediolaterally at the distal end and ranges from 20 mm to 11 mm dorso-ventrally (Fig. 19D, 20D). The ungual is gently recurved ventrally and mediolaterally compressed. The medial side is convex and exceptionally rugose, with a medial ridge running anteroposteriorly, and ridges, grooves and tiny pits across the entire medial surface. The lateral side is much smoother and convex, with some pitting on the dorsal and ventral margins. The dorsal margin is a sharp, convex ridge whereas the ventral margin is somewhat broader and strongly concave. The proximal face is a concave articular surface that is ovoid in outline. The distal end of the ungual is missing, but generally is a blunt tip.

Dermal Armor

We recognize at least three morphologies of scutes (osteoderms) in the material from the Snyder quarry: wing-like with a dorsal crest, wing-like with spines and no dorsal crest, and round or ovoid with no spines (Fig. 21). NMMNH P-31651 is a wing-like scute with a moderately developed crest (Fig. 21A). This scute is small, being 34 mm mediolaterally, 21 mm anteroposteriorly along the medial border, and 18 mm long anteroposteriorly along the lateral edge. The anterior edge is thin with a weakly developed bar that thickens medially. The lateral edge is short and very thin with very delicate spines protruding laterally. The scute body is gently flexed so that the lateral margin dips more ventrally than the medial margin. The posterior edge of the scute is thin, and thickens as it approaches the crest. The posterior margin angles posteriorly from the lateral margin towards the scute's crest, then turns abruptly posteriorly, then medially to the medial margin. The medial margin is thicker than the other edges of the scute, with a shallow, asymmetrical fossa towards the anterior margin. There is a small hook-like process over the anterior margin of this fossa. The dorsal surface bears an ornamentation consisting of a low crest running anteroposteriorly on the medial half of the scute body and several pits. Three deep pits and one shallow, smaller pit are immediately medial of the crest, and there are two or three shallow grooves immediately lateral of the crest. The medial side of the crest is higher and drops abruptly into the pits, whereas the lateral side of the crest slopes gently to the lateral margin. The lateral part of the dorsal surface is lightly striated. The ventral surface is striated and concave, with the line of flexure paral-

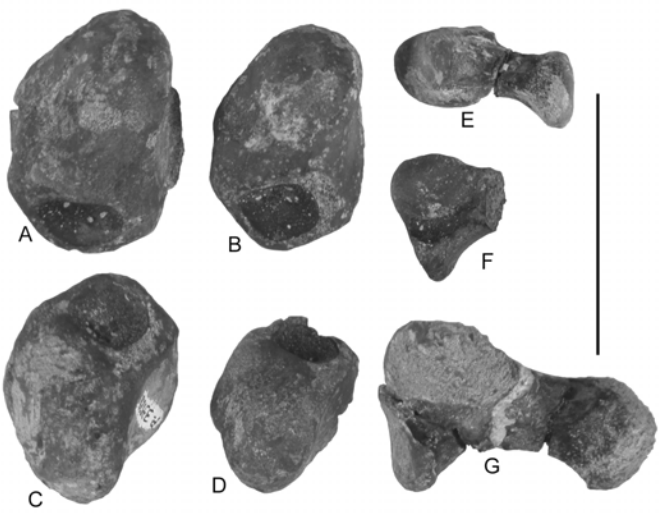

FIGURE 17. Tarsals of *Pseudopalatus* from the Snyder quarry in ventral view. **A**, NMMNH P-33929, right astragalus; **B**, NMMNH P-33856, right astragalus; **C**, NMMNH P-33928, left astragalus; **D**, NMMNH P-33926, left astragalus; **E**, NMMNH P-34753, calcaneum; **F**, NMMNH P-33930, calcaneum; **G**, NMMNH P-39204, calcaneum. Scale bar = 5 cm.

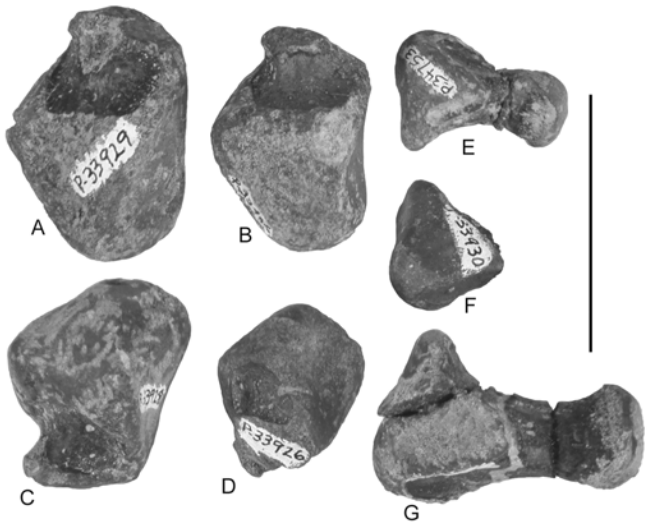

FIGURE 18. Tarsals of *Pseudopalatus* from the Snyder quarry in dorsal view. **A**, NMMNH P-33929, right astragalus; **B**, NMMNH P-33856, right astragalus; **C**, NMMNH P-33928, left astragalus; **D**, NMMNH P-33926, left astragalus; **E**, NMMNH P-34753, calcaneum; **F**, NMMNH P-33930, calcaneum; **G**, NMMNH P-39204, calcaneum. Scale bar = 5 cm.

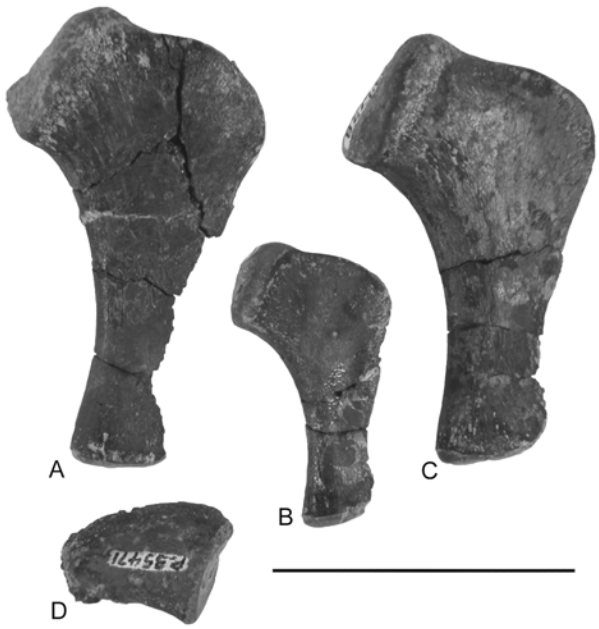

FIGURE 19. Metatarsals of *Pseudopalatus* from the Snyder quarry. **A**, NMMNH P-35796, metatarsal V; **B**, NMMNH P-32129, metatarsal V; **C**, NMMNH P-34728, metatarsal V; **D**, NMMNH P-35471, ungual. Scale bar = 5 cm.

FIGURE 20. Metatarsals of *Pseudopalatus* from the Snyder quarry (opposite side from Fig. 19). **A**, NMMNH P-35796, metatarsal V; **B**, NMMNH P-32129, metatarsal V; **C**, NMMNH P-34728, metatarsal V; **D**, NMMNH P-35471, ungual. Scale bar = 5 cm.

leling the crest on the dorsal surface. On much larger specimens, the dorsal crest can rise up to 5 mm above the scute body and forms a narrow ridge.

NMMNH P-39252 is a scute that is wing-like or ovoid in outline, with more pronounced spines than P-31651, but lacks the dorsal crest (Fig. 21B). This scute is 70 mm in the longest dimension and 35 mm in the shortest dimension. A similar scute that has been fully prepared is 12 mm thick. The delicate spines radiate from all margins of the scute, and we interpret this to mean that these scutes could not have overlapped any neighboring dermal armor. The center of the dorsal surface is ornamented with very small, round pits and is finely striated along the margins. The spines are circular in cross-section and are evenly spaced. A few of the spines are bifurcated near their bases. The ventral side of the scute is smooth with some faint striations, and it is very gently concave.

The third example of a phytosaur scute, NMMNH P-35804, is a round scute that is 44 mm in the longest dimension (mediolateral), 37 mm in the shortest dimension (anteroposterior) and 3-7 mm thick (Fig. 21C). Other scutes similar to this specimen are either round, rounded squares, or tear-drop shaped in outline. The lateral edge of the scute has moderately deep, semi-circular pits that continue halfway along the an-

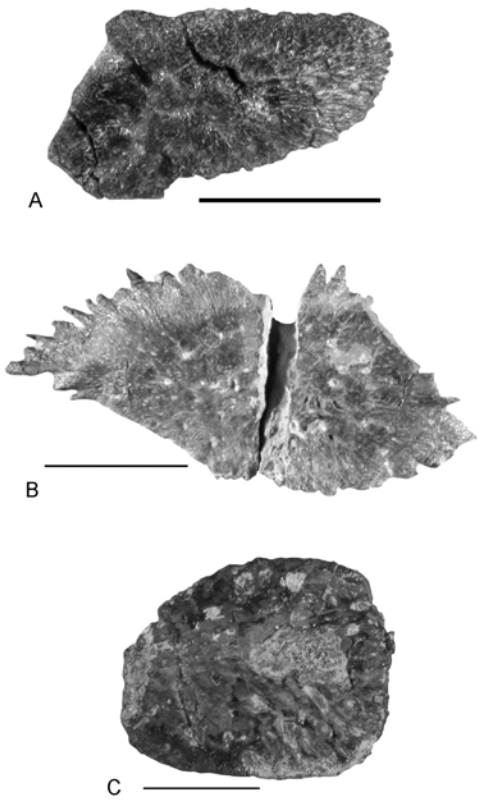

FIGURE 21. Phytosaur scutes (dorsal view) of *Pseudopalatus* from the Snyder quarry. **A**, NMMNH P-31651; **B**, NMMNH P-39252; **C**, NMMNH P-35804. Scale bar = 2 cm.

terior and posterior sides. There are no pits on the medial side, where we assume the scute is overlapped by its neighbor. The scute body swells medially, but there is no distinct boss or ridge. The ventral side is smooth and concave, with a line of flexure that runs anteroposteriorly. There may also be a very faint bar on the anterior side of the scute that is somewhat rougher, and has smaller pitting that the posterior side.

DISCUSSION

This detailed examination of selected phytosaur postcrania is not only useful for simple descriptive purposes, but also may be used to calculate minimum numbers of individuals (MNIs) for the Snyder quarry assemblage. MNIs are useful for establishing relative proportions of taxa within an assemblage, and for a catastrophic assemblage, MNIs can be used to develop a picture of ecosystem dynamics. Here we systematically examine each group of postcranial elements and consider MNIs and possible pairs in each set.

Within the prepared scapulae and coracoids (Fig. 4), there are three scapulae of dramatically different sizes. Regardless of which side each of these scapulae is from, left or right, the differences in size preclude any two of these scapulae being from the same individual. Similarly, there are three left coracoids out of the five specimens, which would lead to an MNI of three. However, one of the right coracoids is much larger than any of the left coracoids and thus the MNI can now be revised to four individuals. When examining these groups of bones for possible pairs, we have only considered a pair to be a left and a right of the same size (within 5 mm difference). Among the coracoids, P-36508 (right, Fig. 2D) and P-37290 (left, Fig. 2G) are of comparable size, despite neither specimen being complete. Also, the large left scapula (P-35998, Fig. 2B) is proportional in size to the large proximal right coracoid (P-36062, Fig. 2E).

In examining the suite of humeri recovered from the Snyder quarry (Figs. 4, 5), there are no immediately apparent good matches between lefts and rights. Thus, with two left and five right humeri of different sizes, our phytosaur MNI based on humeri is seven. The ulnae (Figs. 6, 7), however, reveal at least four, if not five, potential left-right pairs: largest right (P-34756, Fig. 6A) and left (P-31294, Fig. 6G), next largest right (P-35476, Fig. 6B) and left (P-29986, Fig. 6E), intermediate size right (P-33295, Fig. 6C) and left (P-37810, Fig. 6D, and the smallest right (P-34724, Fig. 6I) and left (P-33292, Fig. 6J). It is also possible that P-36410 (right, Fig. 6G) and P-39197 (left, Fig. 6K) are a pair, but given that both are incomplete, this is much less certain. With seven right ulnae, four of which may be paired with matching left ulnae, this yields an MNI of seven.

The radii are less useful, given that P-34749 (Fig. 8A) is the distal end of a right radius and P-34750 (Fig. 8B) is the proximal end, also of a right radius. It is entirely possible that these are two fragments of a single radius, or they could just as easily represent two different radii of comparable sizes. We will use the conservative MNI of one for this set of bones.

The femora from the Snyder quarry are more complex. There are five left femora, four of which are the same size, and three right femora (Figs. 11, 12). None of the lefts and rights are of equivalent sizes, so we can assume an MNI of eight. With four femora of nearly identical proportions, it is highly likely that at least one of these bones was from a phytosaur with a different skull morphology than the others. This implies that the postcrania associated with the two skull morphs cannot be distinguished from each other and this is further evidence that these phytosaurs, despite the different skull morphologies, are the same taxon, and are not two different taxa occupying different ecological niches. The similarity of these femora implies also that the bulk of the variation within *P. buceros* is in the skull and is not as clearly evident in the postcrania.

In examining the tibiae, only one specimen is complete, so matching lefts to rights is tentative at best. Potential pairs are: P-33669 (right, Fig. 13B) and P-36489 (left, Fig. 13F), P-29979 (right and left, Fig. 13C,E), and P-29978 (right, Fig. 13D) and P-37286 (left, Fig. 13G). Because any tibia pairs are tentative, we calculate a MNI of four, based on four right tibiae. Only three fibulae have been recovered so far, two left and one right. P-37352 (right, Fig. 15A) and P-33665 (left, Fig. 15B) are a potential pair. Thus, the MNI based upon fibulae is two. A MNI based upon astragali would be three, based on one large astragalus (P-33929, Fig. 17A), one potential pair (P-33856 and P-33928, Fig. 17B-C), and one small left (P-33926, Fig. 17D).

We also attempted to construct histograms and scatter plots to examine the relationship between bone length and midshaft width for limb bones, given the large number of postcranial elements available for study. However, no definitive relationship was evident for the humeri, ulnae or femora, which have the largest sample sizes. Qualitatively, it appears that the midshaft thickens more than the bone lengthens. This differential growth pattern is more apparent in the proximal limbs (humerus and femur) and less so in the collection of ulnae. This thickening of the midshaft may be related to the need to support the greater weight of an adult animal with a sprawled posture (for discussion of phytosaur body mass, see Hurlburt et al., this volume).

Overall, however, the Snyder quarry phytosaur material appears more gracile than similarly sized phytosaur material from equivalent and younger strata. This difference in robustness may reflect ecological niche partitioning among phytosaur genera (e.g. Hunt, 1989). This large sample of postcrania also reveals a lack of differentiation between the two morphs, as well as few changes during limb growth.

ACKNOWLEDGMENTS

We thank the New Mexico Friends of Paleontology for their exca-

vation and preparation efforts. Funding for work at the Snyder quarry was provided by the Society of Vertebrate Paleontoloy (Bryan Patterson award to ABH), New Mexico Geological Society (Grants-in-aid to KEZ) and the New Mexico Friends of Paleontology. Robert Sullivan and Adrian Hunt provided helpful comments on an earlier draft of this manuscript.

REFERENCES

Ballew, K.L., 1989, A phylogenetic analysis of the Phytosauria from the Late Triassic of the western United States: *in*, Lucas, S.G., and Hunt, A.P., eds., Dawn of the Age of the Dinosaurs in the American Southwest: Albuquerque, New Mexico Museum of Natural History, p. 309-339.

Camp, C.L., 1930, A study of the phytosaurs with description of new material from western North America, Memoirs of the University of California, v. 10, 174 p.

Chatterjee, S., 1978, A primitive parasuchid (phytosaur) reptile from the Upper Triassic Maleri Formation of India: Palaeontology, v. 21, p. 83-127.

Cope, E.D., 1881, *Belodon* in New Mexico: American Naturalist, v. 15, p. 922-923.

Gregory, J.T., 1962, The genera of phytosaurs: American Journal of Science, v. 260, p. 652-690.

Heckert, A.B. and Lucas, S.G., 2000, Phytosaurs (Archosauria: Crocodylotarsi) from the Upper Triassic Owl Rock Formation, Arizona, and their biochronological significance: Mesa Southwest Museum, Bulletin 7, p. 37.

Heckert, A.B., Zeigler, K.E., Lucas, S.G., Rinehart, L.F. and Harris, J.D., 2000, Preliminary description of coelophysoids (Dinosauria: Theropoda) from the Upper Triassic (Revueltian: early-mid Norian) Snyder quarry, north-central New Mexico: New Mexico Museum of Natural History and Science, Bulletin 17, p. 27-32.

Heckert, A.B., Lucas, S.G., Hunt, A.P. and Harris, J.D., 2001, A giant phytosaur (Reptilia: Archosauria) skull from the Redonda Formation (Upper Triassic: Apachean) of east-central New Mexico: New Mexico Geological Society, Guidebook 52, p. 171-178.

Huene, F. v., 1915, On reptiles of the New Mexican Trias in the Cope collection: American Museum of Natural History Bulletin, v. 34, p. 485-507.

Hungerbuhler, A., 2000, Heterodonty in the European phytosaur *Nicrosaurus kapffi* and its implications for the taxonomic utility and functional morphology of phytosaur dentitions: Journal of Vertebrate Paleontology, v. 20, p. 31-48.

Hunt, A.P., 1989, Cranial morphology and ecology among phytosaurs: *in*, Lucas, S.G., and Hunt, A.P., eds., Dawn of the Age of the Dinosaurs in the American Southwest: Albuquerque, New Mexico Museum of Natural History, p. 349-354.

Hunt, A.P., 1994, Vertebrate paleontology and biostratigraphy of the Bull Canyon Formation (Chinle Group, Upper Triassic), east-central New Mexico with revisions of the families Metoposauridae (Amphibia: Temnospondyli) and Parasuchidae (Reptilia: Archosauria) [Ph.D. Dissertation]: Albuquerque, University of New Mexico, 404 p.

Hunt, A.P. and Downs, A.D., 2002, A preliminary taphonomy of the Late Triassic Canjilon Quarry (Petrified Forest Formation, Chinle Group), north-central New Mexico: New Mexico Museum of Natural History and Science, Bulletin 21, p. 291-295.

Hunt, A.P. and Lucas, S.G., 1993, Stratigraphy and vertebrate paleontology of the Chinle Group (Upper Triassic), Chama basin, north-central New Mexico: New Mexico Museum of Natural History and Science, Bulletin 2, p. 61-69.

Hurlburt, G. R., Heckert, A.B. and Farlow, J.O., 2003, Body mass estimates of phytosaurs (Archosauria: Crocodylotarsi) from the Petrified Forest Formation (Chinle Group: Revueltian) based on skull and limb bone measurements: New Mexico Musuem of Natural History and Science, Bulletin 24, p. 105-113.

Kirby, R.E., 1989, Late Triassic vertebrate localities of the Owl Rock Member (Chinle Formation) in the Ward Terrace area of northern Arizona: *in* Lucas, S.G. and Hunt, A.P., eds., Dawn of the Age of the Dinosaurs in the American Southwest, p. 12-28.

Kirby, R.E., 1991, A new vertebrate fauna from the Upper Triassic Owl Rock Member of the Chinle Formation in northern Arizona [M.S. thesis]: Flagstaff, University of Northern Arizona, 476 p.

Kirby, R.E., 1993, Relationships of Late Triassic basin evolution and faunal replacement events in the Southwestern United States: Perspectives from the upper part of the Chinle Formation in northern Arizona: New Mexico Museum of Natural History and Science, Bulletin 3, p. 233-242.

Lawler, D.A., 1974, Osteological variation in the phytosaur *Rutiodon tenuis* from Ghost Ranch, New Mexico [M.S. thesis]: Berkeley, University of California, 140 p.

Long, R.A. and Murry, P.A., 1995, Late Triassic (Carnian and Norian) tetrapods from the southwestern United States: New Mexico Museum of Natural History Bulletin and Science, v. 4, 254 p.

Long, R.A., Lucas, S.G., Hunt, A.P. and McCrea, R.T., 1989, Charles Camp: Collecting Late Triassic vertebrates in the American southwest during the 1920's and 1930's: *in* Lucas, S.G. and Hunt, A.P., eds., Dawn of the Age of the Dinosaurs in the American Southwest: Albuquerque, New Mexico Museum of Natural History, p. 65-71.

Lucas, S.G. and Hunt, A.P., 1992, Triassic stratigraphy and paleontology, Chama basin and adjacent areas, north-central New Mexico: New Mexico Geological Society, Guidebook 43, p. 151-172.

Lucas, S.G., Heckert, A.B., Zeigler, K.E., and Hunt, A.P., 2002, The type locality of *Belodon buceros* Cope, 1881, a phytosaur (Archosauria: Parasuchidae) from the Upper Triassic of north-central New Mexico: New Mexico Museum of Natural History and Science, Bulletin 21, p. 189-192.

Lucas, S.G., Zeigler, K.E., Heckert, A.B., and Hunt, A.P., 2003, Upper Triassic stratigraphy and biostratigraphy, Chama basin, north-central New Mexico: New Mexico Museum of Natural History and Science, Bulletin 24, p. 15-39.

Martz, J.W., 2002a, A new map for the Late Triassic Canjillon quarry (Petrified Forest Member, Chinle Formation), and the ontogeny of *Typothorax coccinarum* (Archosauria, Stagonolepididae): Journal of Vertebrate Paleontology, v. 22, no. 3, p. 84A.

Martz, J.W., 2002b, The morphology and ontogeny of *Typothorax coccinarum* (Archosauria: Stagonolepididae) from the Upper Triassic of the American Southwest [M.S. thesis]: Lubbock, Texas Tech University, 279 p.

McGregor, J.H., 1906, The Phytosauria, with especial reference to *Mystriosuchus* and *Rhytiodon*: Memoirs of the American Museum of Natural History: v. 9, p. 30-110.

Parrish, J.M., 1986, Locomotor adaptations in the hindlimbs and pelvis of the Thecodontia: Hunteria, v. 1, 35 p.

Sullivan, R.M. and Lucas, S.G., 1999, *Eucoelophysis baldwini*, a theropod dinosaur from the Upper Triassic of New Mexico, and the status of the original types of *Coelophysis*: Journal of Vertebrate Paleontology, v. 19, p. 81-90.

Westphal, F., 1976, Phytosauria: Handbuch der Palaoherpetologie, v. 13, p. 99-120.

Zeigler, K.E., 2002, A taphonomic analysis of a fire-related Upper Triassic fossil assemblage [M.S. thesis]: Albuquerque, University of New Mexico, 124 p.

Zeigler, K.E., 2003, Taphonomic analysis for the Snyder quarry: A fire-related Upper Triassic vertebrate fossil assemblage from north-central New Mexico, New Mexico Museum of Natural History and Science, Bulletin 24, p. 49-62.

Zeigler, K.E., Lucas, S.G. and Heckert, A.B., 2002a, A phytosaur skull from the Upper Triassic Snyder quarry (Petrified Forest Formation, Chinle Group) of north-central New Mexico: New Mexico Museum of Natural History and Science, Bulletin 21, p. 171-177.

Zeigler, K.E., Lucas, S.G. and Heckert, A.B., 2002b, The Late Triassic Canjilon quarry (Upper Chinle Group, New Mexico) phytosaur skulls: Evidence of sexual dimorphism in phytosaurs: New Mexico Museum of Natural History and Science, Bulletin 21, p. 179-188.

APPENDIX 1—METRICS OF PHYTOSAUR POSTCRANIA

These tables include all measurements that were possible to make on all specimens listed in Table 1. Schematic diagrams and explanations of all measurements are listed in Appendix 2 (all measurements in mm). *np = not present, n.c. = not complete, (L) = left, (R) = right.

Scapula:

Specimen ID	Total Height	Height of Blade	Length of Blade	Length of Ventral	Width of Blade	Width of Art. Surf.	Dimensions of Glenoid	Dimensions of Acrom. Proc.
P-35998 (L)	258	141	70	88	3	28	53x31	13x28x7
P-35547 (L) (n.c.)	71	35	21	24	7	27	18x16	np
P-36490 (R) (n.c.)	84	42	24	34	6	30	19x17	np

Coracoid:

Specimen ID	Total Length	Length of Art. Surf.	Total Height	Height of Art. Plat.	Width of Ventral Blade	Width of Art. Surf.	Dimensions of Coracoid Notch	Dimensions of Post. Notch
P-37889 (L)	88	53	75	21	2	27	22x24	15x11
P-37290 (L)	nc	61	48	32	3	30	19xnp	np
P-36507 (L)	nc	38	47	25	4	22	np	np
P-36062 (R)	nc	77	47	47	8	46	np	np
P-36508 (R)	nc	62	30	30	4	27	12xnp	np

Humerus:

Specimen ID	Total Width	Length Prox. Head	Height Prox. Head	Length Mid-shaft	Height Mid-shaft	Length Distal Head	Width Distal Head	Length Deltoid Crest	Width Deltoid Crest	Dimensions Ant. Condyle	Dimensions Post. Condyle
P-34733 (L)	131	47	10	14	11	37	12	37	7	14x13	17x12
P-35443 (L)	136	np	np	39	22	np	np	np	np	np	np
P-34751 (L)	118	50	14	16	13	np	np	34	7	np	np
P-29167 (L)	250	99	28	35	25	81	24	85	9	38x32	42x27
P-31297 (R)	169	63	15	20	15	52	16	47	8	21x18	31x18
P-34731 (R)	151	56	15	18	13	45	14	41	9	20x19	24x15
P-36069 (R)	145	58	13	19	15	np	np	40	7	np	np
P-36057 (R)	41	np	np	np	np	43	12	np	np	16x16	24x14

Ulna:

Specimen ID	Total Height	Width of Prox. Head	Length of Prox. Head	Width of Midshaft	Length of Midshaft	Width of Distal Head	Length of Distal Head	Dimensions of Olecranon Proc.
P-31294 (L)	178	58	22	25	12	44	20	26x38x21
P-29986 (L)	145	48	18	24	11	34	9	12x33x14
P-33292 (L)	86	25	7	10	5	18	4	9x12x6
P-39197 (L)	111	np	np	16	9	29	8	np
P-35479 (L)	85	59 (n.c.)	24	np	np	np	np	25x44x19
P-37890 (L)	50	np	np	12	5	20	5	np
P-39253 (L)	146	48	19	19	10	35	8	13x34x18
P-34756 (R)	182	59	19	25	11	39	10	22x37x12
P-35476 (R)	159	50	19	24	10	32	8	19x32x13
P-34724 (R)	49	25	8	11	4	np	np	6x18x8
P-33295 (R)	147	48	18	20	10	36	8	14x36x14
P-36140 (R)	51	34	14	np	np	np	np	10x21x11

Radius:

Specimen ID	Total Height	Width Prox. Head	Length Prox. Head	Width Midshaft	Length Midshaft	Width Distal Head	Length Distal Head
P-34750 (R)	44	np	np	14	11	23	20
P-34749 (R)	112	27	18	16	12	np	np

Fifth Metatarsal:

Specimen ID	Total Length	Width Prox. Head	Height Prox. Head	Width Distal Head	Height Distal Head	Length Med. Branch	Height Med. Branch
P-33129	44	25	3	10	7	16	11
P-34728	65	39	4	18	8	24	18
P-35796	72	39	4	15	9	27	16

Pubis:

Specimen ID	Total Height	Length Dorsal End	Length Ventral End	Width Dors. Keel	Width Vent. Keel	Width Center Keel	Dimensions Obdur. Foram	Dimensions Art. Surf.
P-37346 (R)	137	47 (n.c.)	48 (n.c.)	31	10	21	np	47x34

Ischium:

Specimen ID	Total Height	Length Dorsal End	Length Ventral End	Length Midbone	Width Keel	Width Ant. Blade	Width of Vent. Blade	Dimensions of Art. Surf.
P-34977 (R)	122	64 (n.c.)	68 (n.c.)	36 (n.c.)	23	7	8	41x65

Femur:

Specimen ID	Total Width	Length Prox. Head	Height Prox. Head	Length Midshaft	Height Midshaft	Length Distal Head	Width Distal Head	Width 4th Troch.	Length 4th Troch.
P-34732 (L)	280	72	28	37	25	60	28	65	10
P-33663 (L)	219	55	24	27	22	45	21	44	6
P-30843 (L)	297	77	33	34	27	64	26	64	6
P-37291 (L)	61	np	np	9	8	17	11	np	np
P-35999 (L)	290	80	31	42	24	60	26	55 (n.c.)	9
P-33670 (L)	284	78	34	39	28	65	26	66	8
P-34747 (L)	114	np	np	25	19	np	np	44	5
P-39362 (R)	106	np	np	25	21	53	36	np	np

Femur (cntd.):

Specimen ID	Dimensions Lat. Cond.	Dimensions Med. Cond.	Dimensions 5th Troch.
P-34732 (L)	39x26	35x29	48x5
P-33663 (L)	28x24	29x20	np
P-30843 (L)	44x32	40x26	44x7
P-37291 (L)	10x6	11x8	np
P-35999 (L)	45x32	41x27	40x6 (n.c.)
P-33670 (L)	45x36	41x29	50x6
P-34747 (L)	np	np	28x5
P-39362 (R)	38x24	38x28	np

Tibia:

Specimen ID	Total Height	Width Prox. Head	Length Prox. Head	Width Midshaft	Length Midshaft	Width Distal Head	Length Distal Head	Dimensions of Cnemial Crest
P-36489 (L)	88	51	40	27	21	np	np	np
P-37286 (L)	86	np	np	25	21	41	29	np
P-29979a (R)	80	np	np	22	19	36	31	np
P-29979b (R)	108	np	np	26	21	39	28	np
P-35785 (R)	179	63	44	29	20	45	34	37x6
P-29987 (R)	76	46	35	23	19	np	np	np
P-33669 (R)	151	50	30	25	21	np	np	np

Fibula:

Specimen ID	Total Height	Width Prox. Head	Length Prox. Head	Width Midshaft	Length Midshaft	Width Distal Head	Length Distal Head	Dimensions of Iliofib. Troch.
P-37358 (L)	124	18	10	11	9	24	13	19x7
P-39363 (L)	182	27	16	18	14	38	20	25x10
P-37352 (R)	174	28	17	18	14	38	19	26x13
P-39364 (R)	44	np	np	16	9	29	9	np

Astragalus:

Specimen ID	Total Length	Width Ant. End	Height Ant. End	Width of Midbone	Height of Midbone	Width Post. End	Height Post. End	Dimensions Metatarsal Facet	Dimensions Tibial Saddle
P-33929 (L)	46	23	16	30	30	21	23	15x11	22x14
P-33856 (L)	41	20	17	26	27	19	24	14x11	17x10
P-33926 (R)	30	19	13	22	22	17	22	12x8	16x10
P-33928 (R)	40	22	17	28	28	18	24	13x14	20x12

Calcaneum:

Specimen ID	Total Width	Length Lat. End	Height Lat. End	Length Midbone	Height Midbone	Length Med. End	Heightd Med. En	Dimen. Ventr. Anter. Facet	Dimensions Post. Triang. Facet
P-34753 (L)	33	14	15	9	9	7	23	16x9x14	15x19
P-39204 (R)	50	21	18	14	14	13	30	22x14x19	24x28
P-33930 (R)	20	np	np	np	np	20	10	18x11x15	15x20

Distal Ungual:

Specimen ID	Total Length	Width Prox. End	Height Prox. End	Width of Midbone	Height of Midbone	Width Distal End	Height Distal End
P-35471 (L?)	27 (n.c.)	11	20	10	17	6	11

APPENDIX 2—BONE MEASUREMENT PROTOCOLS

Here we schematically diagram the measurements that were taken on each bone. Height = ventral-dorsal measurement, length = anterior-posterior measurement, width = medial-lateral measurement. Note that because of the orientation of the proximal limb elements (humerus and femur) in a sprawled posture that the "length" of the bone from proximal to distal end is the same as the medial to lateral width of the bone.

A. Scapula: a = height, b = height of blade, c = length across blade top, d = length across base, e = width of blade, f = width across widest part of articular surface, g = dimensions of glenoid, h = dimensions of acromion process.

B. Coracoid: a = length, b = length of articular platform, c = height, d = height of articular platform, e = width of ventral blade, f = width of widest part of articular platform, g = dimensions of articular facet, h = dimensions of coracoid notch, i = dimensions of posterior notch.

C. Humerus: a = width (proximal - distal length), b = length of proximal head, c = height of proximal head, d = length of midshaft, e = height of midshaft, f = length of distal head, g = height of distal head, h = width of deltoid crest, i = length of deltoid crest, j = dimensions of distal condyles.

D. Ulna: a = height, b = width of proximal head, c = length of proximal head, d = width of midshaft, e = length of midshaft, f = width of distal head, g = length of distal head, h = dimensions of olecranon process.

E. Radius: a = height, b = width of proximal head, c = length of proximal head, d = width of midshaft, e = length of midshaft, f = width of distal head, g = length of distal head.

F. Pubis: a = height, b = length of ilial articular surface, c = length of ventral surface, d = width of dorsal end of keel, e = width of ventral end of keel, f = width of center of keel, g = dimensions of obdurator foramen, h = dimensions of ilial articular surface.

G. Ischium: a = height, b = length of ilial articular surface, c = length of ventral surface, d = length of midbone, e = width of keel, f = width of anterior blade, g = width of ventral blade, h = dimensions of ilial articular surface.

H. Femur: a = width of bone (distal - proximal length), b = length of proximal head, c = height of proximal head, d = length of midshaft, e = height of midshaft, f = length of distal head, g = height of distal head, h = width of 4^{th} trochanter, i = length of 4^{th} trochanter, j = dimensions of lateral condyle, k = dimensions of medial condyle, l = dimensions of 5^{th} trochanter.

I. Tibia: a = height, b = width of proximal head, c = length of proximal head, d = width of midshaft, e = length of midshaft, f = width of distal head, g = length of distal head, h = dimensions of cnemial crest.

J. Fibula: a = height, b = width of proximal head, c = length of proximal head, d = width of midshaft, e = length of midshaft, f = width of distal head, g = length of distal head, h = dimensions of iliofibular trochanter.

K. Astragalus: a = length, b = width of anterior end, c = height of anterior end, d = width of midbone, e = height of midbone, f = width of posterior end, g = height of posterior end, h = dimensions of metatarsal facet, i = dimensions of tibial saddle.

L. Calcaneum: a = width, b = length of lateral end, c = height of lateral end, d = length of midbone, e = height of midbone, f = length of medial end, g = height of medial end, h = dimensions of ventral articular facet, i = dimensions of posterior triangular facet.

M. Vth Metatarsal: a = length, b = width of proximal head, c = height of proximal head, d = width of distal head, e = height of distal head, f = length of medial branch, g = height of medial branch.

N. Ungual: a = length, b = width of proximal end, c = height of proximal end, d = width of midbone, e = height of midbone, f = width of distal end, g = height of distal end.

O. Scutes: a = length, b = width, c = height, d = dimensions of any crest or ornamentation.

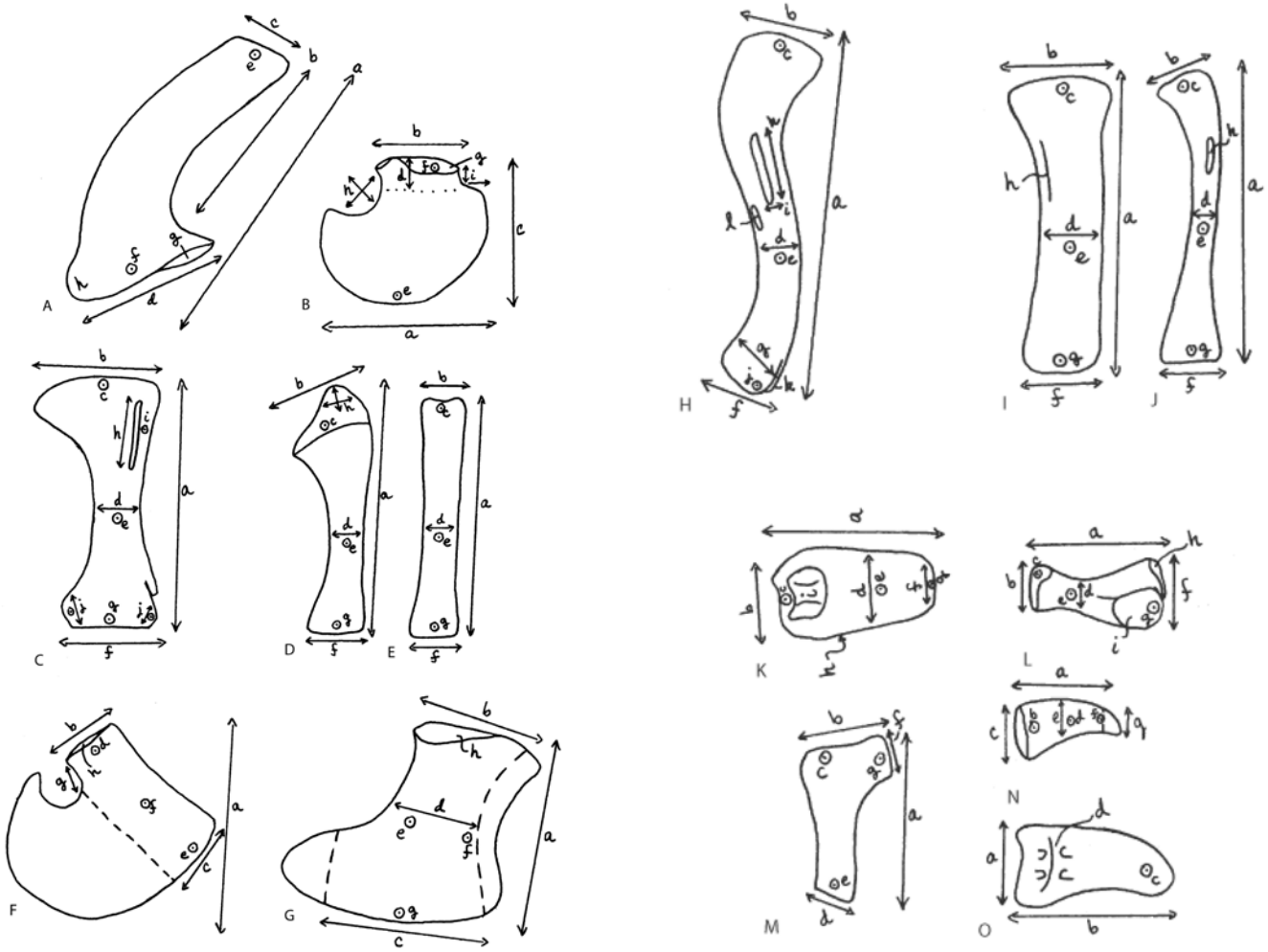
A
B
C
D
E
F
G
H
I
J
K
L
M
N
O

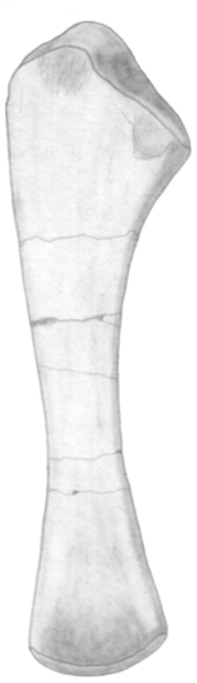

NMMNH P-33292, a left ulna of the phytosaur *Pseudopalatus buceros* from the Snyder quarry (illustration by K.E. Zeigler).